Table IV. Selective Hydrogenation of 1,3-Cyclohexadiene—Effect of Catalysts, Pressure, and Solvents[a]

catalyst	solvent	initial H_2 pressure (psi)	inductn time (h)	convn (%)	turnover rate (mol/mol of Pd·h)	products (%) cyclohexene	products (%) cyclohexane	selectivity[b] (%)
$FeCpC_5H_3(CH_2NMe_2)$-[S(*t*-Bu)$PdCl_2$	acetone	102.0	2.8	100	61.0	46.9	53.1	46.9
$FeCpC_5H_3(CH_2NMe_2(SPh)$-$PdCl_2$	acetone	65.0	4.5	100	268.9	66.8	33.2	66.8
	acetone	102.0	1.5	100	936.8	64.3	35.7	64.3
$FeCpC_5H_3(CH_2NMe_2)$-[S(4-tolyl)]$PdCl_2$	acetone	102.0	2.8	100	1005.0	62.1	37.9	62.1
	acetone/methylene chloride (1:2)	102.0	47.3	96.4	18.8	93.5	2.9	97.0
	methylene chloride	102.0		no H_2 uptake				

[a] 9.0 mL of solvent, 2.0×10^{-5} mol of catalyst, 7.40×10^{-3} mol of substrate, room temperature. [b] Cyclohexane (cyclohexane + cyclohexene).

Table V. Homogeneous Selective Hydrogenation of Dienes to Monoenes[a]

initial rate (mol/mol of Pd·H·psi)	substrate	*T*, °C	metal	solv	ref
3.38	1,3-COD	27	Pd^{2+} (**25**)	acetone	this work
4.90	1,3-COD	27	Pd^{2+} (**20**)	acetone	this work
5.66	1,3-COD	27	Pd^{2+} (**23**)	acetone	this work
11.33	1,3-COD	27	Pd^{2+} (**27**)	acetone	this work
10.83	1,3-cyclohexadiene	27	Pd^{2+} (**25**)	acetone	this work
11.82	1,3-cyclohexadiene	27	Pd^{2+} (**27**)	acetone	this work

[a] COD = cyclooctadiene. Ligands vary from case to case.

hexadiene to cyclohexene is shown in Table IV. The catalysts and 1,3-cyclohexadiene dissolved completely in methylene chloride and became a red-brown solution. The solution is catalytically inactive since H_2 is unable to add oxidatively to Pd. When the complexes are dissolved in acetone, acetone may replace the thioether in coordinating to Pd, and the substrate is introduced into solution by coordinating to Pd center of the catalyst–acetone intermediate and then H_2 uptake immediately occurs to induce the hydrogenation. In the mixed-solvent acetone and methylene chloride, the hydrogenation turnover rate decreases but the selectivity increases, so the solvent effect is important in the selective hydrogenation of the 1,3-cyclohexadiene. The turnover rate declined in the order **27** > **25** > **23** because the breaking of the Pd–S bond appears to be important to the selective hydrogenation and the electron-withdrawing effect is stronger than the steric (crowding) effect of the alkyl or aryl substituents of the thioether in the palladium ferrocenyl sulfide catalysts. With the same catalyst and solvent (acetone), the turnover rate at 102.0 psi of initial H_2 pressure is 3 times as large as at 65.0 psi of initial H_2 pressure. The results of the selective hydrogenation of 1,3-cyclooctadiene to cyclooctene are compared with those of 1,3-cyclohexadiene to cyclohexene. The turnover rate of the latter is high, but the selectivity of the monoene is comparatively low.

Promotion of Me/CO Migratory Insertion by Transition-Metal Lewis Acids. Synthesis and Reactivity of a Transition-Metal Heterobimetallic Carbonyl Alkyl Anion, $MeFeW(CO)_9^-$

L. W. Arndt, B. T. Bancroft, M. Y. Darensbourg,* C. P. Janzen, C. M. Kim, J. Reibenspies,
K. E. Varner, and K. A. Youngdahl

Department of Chemistry, Texas A&M University, College Station, Texas 77843

Received August 27, 1987

The heterobimetallic alkyl anion 1 was prepared by alkylation of $FeW(CO)_9^{2-}$ using MeI or MeOTs. Addition of the monometallic $MeFe(CO)_4^-$ to a solution of $W(CO)_5$·THF produced the same product. Spectroscopic data indicated the structure of 1 to be analogous to that of $HFeW(CO)_9^-$ or $Ph_3AuFeW(CO)_9^-$, i.e., containing octahedral metal centers with a CH_3 group bound to Fe, cis to the Fe–W bond. A comparative rate study of the reaction of with monomeric $MeFe(CO)_4^-$ and with 1 indicated the promotional effect of $W(CO)_5^0$ for the Me/CO migratory insertion reaction. There was no reaction of $MeFe(CO)_4^-$ with CO_2, whereas bimetallic 1 readily added CO_2 yielding $MeC(O)OW(CO)_5^-$. With CS_2 a heterobimetallic, formulated as μ-$MeCS_2FeW(CO)_8^-$, was produced.

Introduction

The extent to which an adjacent metal influences the reactivity of a functionalized organometallic is of interest with respect to heterobimetallic complex reactivity and reaction pathways. Herein we report the synthesis, structure, stability, and small molecule reactions of $MeFeW(CO)_9^-$ (**1**).

Complex anion **1** is a member of a family of heterobimetallics containing metal–metal bonds that are best described as metal donor–metal acceptor complexes. Other members of that family are $HFeM(CO)_9^-$, $HFeM(CO)_8PR_3^-$ (M = Cr, Mo, W),[1,2] and $Ph_3PAuFeW(CO)_9^-$.[3] As indi-

---

(1) (a) Arndt, L. W.; Delord, T.; Darensbourg, M. Y. *J. Am. Chem. Sco.* **1984**, *106*, 456. (b) Arndt, L. W.; Delord, T.; Darensbourg, M. Y.; Bancroft, B. T. *J. Am. Chem. Soc.* **1986**, *108*, 2617.

(2) Arndt, L. W.; Darensbourg, M. Y. *Inorg. Synth.*, in press.

(3) Arndt, L. W.; Darensbourg, M. Y.; Fackler, J. P.; Lusk, R. J.; Marler, D. O.; Youngdahl, K. A. *J. Am. Chem. Soc.* **1985**, *107*, 7218.

0276-7333/88/2307-1302$01.50/0 © 1988 American Chemical Society

cated below, all may be considered derivatives of the parent mixed-metal dianion $FeM(CO)_9^{2-}$[1a] and electrophiles. Indeed, eq 1 represents in most cases the synthetic procedure of choice. X-ray crystallography established

(1)

a similarity between all structures which permits the group 6 metal to maintain octahedral symmetry by using $EFe(CO)_4^-$ as a metalloligand. The structures of the hydride derivatives were quite different from those of the homobimetallic analogues $(\mu\text{-H})M_2(CO)_{10}^-$[4] and $(\mu\text{-H})Fe_2(CO)_6(\mu\text{-CO})_2^-$;[5] i.e., the homobimetallic anions contain bridging hydrides, no M–M bond in the case of group 6 dimers, and an Fe–Fe bond plus μ-CO's in the case of the iron dimer.

The principal difference in chemical reactivity of $HFeW(CO)_9^-$ or $HFeCr(CO)_9^-$ as contrasted to monomeric $HFe(CO)_4^-$ was a dramatic increase in CO lability. This lability was the presumed reason for the enhanced activity of $HFeM(CO)_9^-$ as an olefin isomerization catalyst, as compared to $HFe(CO)_4^-$.[6]

There was some (small) expectation that the $M(CO)_5$ moiety might promote H/CO migratory insertion in $HFeM(CO)_9^-$. Unfortunately, no experimental evidence was found to support such a prospect. On the other hand, $RFe(CO)_4^-$ anions are well-known for their tendency to undergo R/CO migratory insertion,[7] and such a reaction is described below as a contrast of heterobimetallic and monometallic complex chemistry.

Experimental Section

A. General Data. 1. Procedures. All operations were carried out under nitrogen by using standard Schlenk techniques or an argon-filled glovebox. Rigorous exclusion of trace moisture and oxygen was standard procedure. Solvents were dried and degassed as described below.

2. Equipment. Infrared spectra were recorded on an IBM FTIR/85, IBM FTIR/32, or a Perkin-Elmer 283 spectrophotometer using 0.10-mm sealed CaF_2 solution cells. ^{31}P, ^{13}C, and ^1H NMR spectra were recorded on an XL200 or XL200E Varian spectrometer referenced against H_3PO_4, benzene-d_6, and THF, respectively. Benzene and THF were ultimately referenced against TMS. Gas chromatographs were recorded on a Perkin-Elmer Sigma 2 GC in line with a Perkin-Elmer LCI-100 laboratory computing integrator. A Porapak T column (170 °C, flow rate = 25 mL/min) or a Carbosphere column (200 °C, flow rate = 30 mL/min) was used to detect the presence of low molecular weight alkanes (i.e., methane and ethane). A carbowax column (60 °C, flow rate = 20 mL/min) was used to observe ketones and aldehydes.

B. Materials. 1. General Data. Tetrahydrofuran (THF) and hexane were distilled under nitrogen from sodium/benzophenone ketyl. Acetone was dried over calcium hydride and stored over 3-Å molecular sieves. Acetonitrile was distilled twice from calcium hydride and then twice from P_2O_5 and stored over 3-Å molecular sieves. Diethyl ether was distilled from lithium aluminum hydride. Methylene chloride was refluxed over phosphorus pentoxide and distilled under N_2. Bis(triphenylphosphine)nitrogen(1+) chloride (PPN^+Cl^-) and tetraethylammonium hydroxide ($Et_4N^+OH^-$ in MeOH) were purchased from Aldrich. High grade (99.99%) CO was purchased from Johnson and Matheson. Nitrogen was predried through calcium chloride and calcium sulfate prior to use. $Fe(CO)_5$ (Alfa Products) was stored in a dark bottle under nitrogen and filtered immediately prior to use. All other reagents were purchased from standard vendors as reagent or better grade and used without purification.

2. [PPN][MeFeW(CO)$_9$] (PPN$^+$1). A 0.40-g (2.5-mmol) sample of $[PPN]_2[FeW(CO)_9]$[2] was placed in a 50-mL Schlenk flask and dissolved in 40 mL of dry CH_3CN. Methyl tosylate was liquified at 40 °C, and 0.48 g (2.5 mmol) was quickly added to the bright orange solution by syringe. The stirred solution rapidly turned yellow. The solvent was removed in vacuo yielding a yellow-brown oil. This residue was dissolved in 30 mL of Et_2O and filtered through a Celite-covered glass frit. The solution was concentrated to 10 mL, and hexane was added dropwise to precipitate out a yellow-brown solid. The solid was washed twice with hexane and dried in vacuo. The solid was recrystallized from Et_2O and hexane to give a yellow-orange, crystalline solid with a yield of 1.64 g (62%). Elemental Anal. (Galbraith) Calcd for **PPN$^+$1**, $C_{45}H_{30}NO_9P_2FeW$ (Found): C, 52.85 (52.77); H, 3.18 (3.20); N, 1.34 (1.14). IR (THF): ν(CO) 2060 (w), 2004 (m), 1942 (s), 1909 (m), 1863 (m) cm^{-1}. ^1H NMR (acetone-d_6): δ –0.32 (s, CH_3). ^{13}C NMR (THF and CD_3CN): δ 222.4 ($Fe(CO)_4$), 206.5 ($W(CO)_{ax}$), 206.2 ($W(CO)_{eq}$) (J = 125.6 Hz), –12.3 (CH_3).

3. [Et$_4$N][MeFeW(CO)$_9$] (Et$_4$N$^+$1). Method A. The Et_4N^+ salt of 1 was prepared by the same method as above except with $[Et_4N]_2[FeW(CO)_9]$ as the starting material. **Method B.** A 1.00-g (3.20-mmol) sample of $[Et_4N][MeFe(CO)_4]$ (prepared vide infra) was placed in a 100-mL Schlenk flask. To this was added 90 mL of a 3.56×10^{-2} M (3.20 mmol) solution of $W(CO)_5 \cdot THF$. The resulting yellow-orange solution was stirred for 5 min and then concentrated to 10 mL. Slow addition of 40 mL of hexane resulted in the separation of a yellow-orange oil. After removal of solvent via cannula, this residue was redissolved in 20 mL of THF and filtered through a Celite-covered glass frit. The solution was concentrated to 10 mL, and hexane was added dropwise to precipitate out a orange-yellow solid. The solid was washed twice with hexane and dried in vacuo. Recrystallization from a 1:1 mixture of THF/Et_2O and hexane yielded 1.18 g (58%) of pure product.

4. [Na][MeFeW(CO)$_9$] (Na$^+$1). A 0.050-g (0.048-mmol) sample of **PPN$^+$1** was loaded into a Schlenk tube with 5 equiv (0.24 mmol) of $NaBPh_4$. A 5-mL portion of THF was added via syringe while stirring to produce a yellow heterogeneous solution containing a white precipitate of $[PPN][BPh_4]$. The precipitate was allowed to settle, and the clear yellow supernatant was cannulated off for immediate use in kinetic experiments. Solutions used in situ gave identical results. At least 5 equiv of $NaBPh_4$ was required to effect complete cation exchange. Addition of 10 equiv of $NaBPh_4$ provided identical results, however, addition of 2 equiv of $NaBPh_4$ resulted in an incomplete cation exchange.

5. [PPN][MeFe(CO)$_4$] (PPN$^+$2). A 1.00-g sample of $[PPN][HFe(CO)_4]$[8] (1.41 mmol) was loaded into a 50-mL Schlenk flask and dissolved in 10 mL of freshly distilled THF. This solution was cooled to –78 °C. A 1.5-equiv amount of n-butyllithium (1.6 M in hexane) was added dropwise by syringe until the solution was dark red and a precipitate began to form. The solution was warmed to ambient temperature, and the dark red supernatant solution was cannulated off. The red-brown solid was washed three times with THF and once with hexane. After the mixture was dried in vacuo, 10 mL of THF was added. To this heterogeneous mixture was slowly added 0.29 g (1.58 mmol) of warmed methyl tosylate via syringe. The iron dianion reacted heterogeneously with MeOTs yielding a light brown solution. This solution was filtered through a Celite-covered frit. Ether was added slowly to the filtrate to yield a light tan precipitate. Recrystallization from THF/ether yielded 0.336 g (33%) of a pale yellow crystalline solid. Elemental Anal. (Galbraith) Calcd for **PPN$^+$ 2**, $C_{40}H_{30}NO_4P_2Fe$ (Found): C, 68.25 (68.44); H, 4.61 (4.59). IR (THF): 1991 (mw), 1870 (s) cm^{-1}. ^1H NMR (acetone-d_6): δ 0.16 (s, CH_3). ^{13}C

---

(4) (a) Bau, R.; Teller, R. G.; Kirtley, S. W.; Koetzle, T. F. *Acc. Chem. Res.* **1979**, *12*, 176. (b) Hart, D. W.; Bau, R.; Koetzle, T. F. *Organometallics* **1985**, *4*, 1590. (c) Peterson, J. L.; Brown, R. K.; Williams, J. M. *Inorg. Chem.* **1981**, *20*, 158. (d) Roziere, J.; Teulon, P.; Grillone, M. D. *Inorg. Chem.* **1983**, *22*, 557.

(5) Collman, J. P.; Finke, R. G.; Matlock, P. L.; Wahren, R.; Komoto, R. G.; Brauman, J. I. *J. Am. Chem. Soc.* **1978**, *100*, 1119.

(6) Tooley, P. A.; Arndt, L. W.; Darensbourg, M. Y. *J. Am. Chem. Soc.* **1985**, *107*, 2422.

(7) Collman, J. P.; Finke, R. G.; Cawse, J. N.; Brauman, J. I. *J. Am. Chem. Soc.* **1978**, *100*, 4766.

(8) Darensbourg, M. Y.; Darensbourg, D. J.; Barros, H. L. C. *Inorg. Chem.* **1978**, *17*, 297.

NMR (THF and acetone-d_6): δ 223.56 ($Fe(CO)_4$), 21.38 (CH_3). The Et_4N^+ analogue was prepared in an analogous fashion by using $[Et_4N][HFe(CO)_4]$ as the starting material.

6. $[Na][MeFe(CO)_4]$ (Na^+2). A 5-mL portion of THF was added via syringe to a Schlenk tube containing 0.035 g (0.049 mmol) of **PPN^+2** and 5 equiv (0.24 mmol) of $NaBPh_4$ to yield a light tan heterogeneous solution. The ion exchange occurred as described for 3.

7. $[Et_4N][MeC(O)Fe(CO)_3PPh_3]$ (Et_4N^+3). This compound was prepared by the method described by Casey et al.[9] Recrystallization from acetonitrile and ether yielded large yellow crystals.

C. Kinetics. 1. In a typical study, 0.0485 mmol of 1 or 2 was loaded inside a drybox into a Schlenk tube. The appropriate amount of triphenylphosphine was added. The Schlenk tube was removed from the drybox and placed in a constant temperature bath. After the system had come to thermal equilibrium, 5 mL of THF was syringed into the flask. This solution was agitated until homogeneous. Samples were removed periodically, and the rate was determined by monitoring the disappearance of an isolated carbonyl peak in the infrared spectrum (2006 cm^{-1} for 1 and 1991 cm^{-1} for 2). The sodium salts were prepared in situ as described previously. A 20-fold excess of triphenylphosphine was added, and the solution was agitated briefly. The rates were determined as described above.

2. Analysis of Kinetic Data. Under the pseudo-first-order conditions described, plots of ln $[A_t - A_\infty]$ vs time were linear. Both $MeFeW(CO)_9^-$ and $MeFe(CO)_4^-$ showed a linear phosphine concentration dependence, implicative of an overall second-order reaction. At 25 °C and a 20× excess of PPh_3, the half-life for **PPN^+1** was about 26 min; for **PPN^+2**, the half-life was about 20 h. Pseudo-first-order rate constants were derived from the least-squares fit of the data, and second-order rate constants were calculated: $k_2 = k_{obsd}(av)/[PPh_3]$.

D. Reactions of $MeFeW(CO)_9^-$. 1. Addition of CO. A 50-mg (0.048-mmol) sample of **PPN^+1** was loaded into a 50-mL Schlenk flask, and 15 mL of THF was added. The system was evacuated and back-filled with CO to 1 atm (ca. 0.15 mmol). Over the course of 2 days at room temperature, **PPN^+1** decomposed. The final products, $W(CO)_6$ and $MeC(O)Fe(CO)_4^-$ (4) were identified by infrared solution spectra.

2. Addition of CO_2. A 25-mg (0.024-mmol) sample of **PPN^+1** was loaded into a 50-mL Schlenk flask and dissolved in 5 mL of THF. The flask was evacuated and back-filled with CO_2 to 1 atm. The reaction was monitored by IR, and over the course of 4 days at room temperature, the solution remained yellow; however, a brown precipitate had formed. The solution IR carbonyl spectrum of this yellow solution showed bands at 2059 (w), 1907 (s), and 1843 (m) cm^{-1}, characteristic of $W(CO)_5OC(O)CH_3^-$.[10] An additional band at 1978 (m) cm^{-1} was indicative of $W(CO)_6$. The isolated brown solid was insoluble in polar solvents and was presumed to be iron-containing decomposition products.

3. Addition of CS_2. A 550-mg (0.526-mmol) sample of **Et_4N^+1** was placed in a 50-mL Schlenk flask along with 25 mL of THF. This yellow solution was stirred while 32 μL (0.53 mmol) of CS_2 was added via syringe. The solution was stirred for 1 hour during which the color changed from yellow to green to brown-red. The solvent was removed in vacuo to yield a brown oil. The oil was taken up in Et_2O/THF and passed through an alumina column. Hexane was added slowly to the eluant to precipitate a dark red-brown solid. The solid was washed twice with hexane and dried in vacuo. Recrystallization from THF/hexane yielded 225 mg (62%) of $[Et_4N][(\mu_2\text{-}S_2CMe)FeW(CO)_8]$ (**5**). Elemental Anal. (Galbraith) Calcd for **5**, $C_{18}H_{23}NO_8S_2FeW$ (Found): C, 31.55 (31.38); H, 3.38 (3.31). IR (THF): 2060 (w), 2033 (m), 1976 (m), 1924 (s), 1956 (mw), 1882 (m) cm^{-1}. ^1H NMR: δ 2.11 (s, CH_3).[27]

4. Addition of Acids. An aliquot (50 μL, 0.85 mmol) of CH_3COOH was added to **PPN^+1** (0.050 g, 0.048 mmol) in 1 mL of THF. No color change was noted; however, methane was detected above and in the solution by GC. An unresolved mixture of carbonyl-containing products was observed by IR. Similar results were noted when the acid used was concentrated HCl.

5. Addition of MeI. A 100-μL (0.32-mmol) aliquot of MeI was added to a 10-mL THF solution of **PPN^+1** (0.050 g, 0.048 mmol). The solution was stirred for 1 h under N_2. The GC trace indicated the formation of acetone and some methane as the organic products. $[PPN][W(CO)_5I]$ was the only identifiable organometallic product.

6. Reaction of $[PPN][MeFe(CO)_4]$ with $W(^{13}CO)_5\cdot THF$. A sample (0.10 g, 0.28 mmol) of the ^{13}C isotopically enriched $W(*CO)_6$ (the asterisk (*) = mixture of ^{12}C and ^{13}C) was dissolved in 5 mL of THF in a small photolysis flask. Photolysis for 15 min yielded $W(*CO)_5\cdot THF$. Meanwhile, a 0.20-g (0.28-mmol) sample of **PPN^+2** was placed in a 5-mm NMR tube containing a 0.10-mL portion of benzene-d_6 as a deuterium lock. A vacuum was pulled on the tungsten solution to reduce the volume to <1 mL. This solution was then syringed into the NMR tube containing **PPN^+2** and benzene-d_6. The tube was briefly agitated after which an NMR spectrum was immediately taken. After 64 scans (4.3 min), the spectrum not only revealed large carbonyl peaks at 206.7 and 206.3 ppm ($W(CO)_{eq}$ and $W(CO)_{ax}$ carbons), but also displayed a large peak at 222.7 ppm indicative of the heterobimetallic alkyl species enriched on the iron center, $MeFe(*CO)_4W(*CO)_5^-$.

E. Reactions of $MeFe(CO)_4^-$. 1. Addition of CO_2. A 62-mg (0.086-mmol) sample of **PPN^+2** was placed in a sample vial and dissolved in 15 mL of THF. A 300-mL Parr reactor was evacuated and backfilled with N_2. The THF solution was transferred to the Parr reactor through a cannula. The system was then pressurized to 600 psi with carbon dioxide and stirred at room temperature. The solution, as analyzed by IR, showed no reaction after 24 h.

2. Addition of CH_3COOH. A 0.025-g (0.0346-mmol) sample of **PPN^+2** was dissolved in 1.0 mL of THF to give 0.0346 M solution. Acetic acid (2 μL, 0.0346 mmol) was added via syringe. The tan solution darkened rapidly to an amber brown. This solution was examined by GC to reveal the presence of methane as the exclusive organic product. Infrared spectroscopy indicated decomposition of the carbonyl species.

3. Addition of MeI. To a 0.025-g (0.0346-mmol) sample of **PPN^+2** was added 1.0 mL of THF yielding a 0.0346 M solution. A 2-μL aliquot of MeI was carefully added. A dramatic color change from light tan to dark red was noted immediately. The organic products, methane and acetone, were identified by GC. No ethane was detected. The IR revealed a complex mixture of organometallic products.

4. Addition of CS_2. A 35-mg (0.49-mmol) sample of **PPN^+2** was dissolved in 5 mL of THF to give a pale yellow solution. An excess (0.11 mL, 1.9 mmol) of CS_2 was syringed in resulting in a color change to lemon yellow. An infrared spectrum revealed a clean set of new bands at 1910 (s) and 1841 (m) cm^{-1}. The solvent was concentrated by vacuum, and hexane was added resulting in pale yellow microcrystalline solid. However, as further analysis indicated, this solid was simply the starting material **PPN^+2**.

5. Addition of CO. A 50-mL Schlenk flask was loaded with a 35-mg (0.049-mmol) sample of **PPN^+2** dissolved in 5 mL of THF. The flask was evacuated and backfilled with 1 atm of CO at room temperature. The solution was monitored by IR to note the disappearance of the peak at 1991 cm^{-1} due to the starting material **PPN^+2**. The reaction was rather slow, with the product $[PPN][MeC(O)Fe(CO)_4]$ (ν(CO) = 2048 (w), 1885 (s), and 1586 (m) cm^{-1}) being formed over a 24 h period.

6. Addition of PPh_3. In a 25-mL Schlenk tube, 50 mg (0.069 mmol) of **PPN^+2** was loaded along with 0.36 g (1.39 mmol) of PPh_3. A 5-mL portion of THF was added, and the solution was monitored by IR to follow the disappearance of **PPN^+2**. The phosphine acyl product $[PPN][MeC(O)Fe(CO)_3PPh_3]$ (ν(CO) = 1939 (w), 1851 (s), and 1555 (m) cm^{-1}) was observed during the course of the reaction but eventually decomposed to $[PPN][MeC(O)Fe(CO)_4]$ and an unidentified orange solid iron product. Reaction of **Na^+2** with PPh_3 was accomplished in a similar fashion.

F. Reactions of $MeC(O)Fe(CO)_3PPh_3^-$ (3). 1. Thermal Stability. A 10-mg sample of **Et_4N^+3** was placed in a small ampule and dissolved in CH_3CN. The solution was monitored by IR over a period of days at room temperature to observe the slight decomposition that occurred. After 70 h, 85% of the starting material remained in solution.

---

[9] Casey, C. P.; Meszaros, M. W.; Neumann, S. M.; Cesa, I. G.; Haller, K. J. *Organometallics* **1985**, *4*, 143.

[10] (a) Cotton, F. A.; Darensbourg, D. J.; Kolthammer, B. W. S.; Kudaroski, R. *Inorg. Chem.* **1982**, *21*, 1656. (b) Darensbourg, D. J.; Morse, S. A.; Ovalles, C. *Inorg. Synth.*, submitted for publication.

2. Addition of $W(CO)_5{\cdot}THF$. A 25-mL aliquot (0.11 mmol) of a 0.0045 M solution of $W(CO)_5{\cdot}THF$ was added to a 0.040-mg (0.069-mmol) sample of **Et$_4$N$^+$3**. The solution was stirred briskly and monitored by IR.

3. Addition of CO. A 30-mg (0.052-mmol) sample of **Et$_4$N$^+$3** was loaded into a 100-mL Schlenk flask. A 10-mL portion of THF was added to partially dissolve the solid, yielding a heterogeneous mixture. The flask was evacuated and then charged with 1 atm of CO. This mixture was stirred vigorously and monitored by IR.

Results and Discussion

Synthesis of $MeFeW(CO)_9^-$. The heterobimetallic alkyl may be prepared by two different routes, eq 2 and 3. The first involves reaction of the heterodinuclear dianion $FeW(CO)_9^{2-}$ with either methyl tosylate or methyl iodide to give the alkylated product.

$$FeW(CO)_9^{2-} + MeI \text{ or } MeOTs \rightarrow MeFeW(CO)_9^- \tag{2}$$

$$MeFe(CO)_4^- + W(CO)_5{\cdot}THF \rightarrow MeFeW(CO)_9^- \tag{3}$$

Methyl tosylate was preferred as excess methyl iodide induced further reaction with $MeFeW(CO)_9^-$ to generate acetone and metal decomposition products. The second route, aggregation of the monomeric alkyl $MeFe(CO)_4^-$ with $W(CO)_5{\cdot}THF$, involves the replacement of the labile ligand THF with the metalloligand $MeFe(CO)_4^-$. This latter method was not as efficient due to contamination of the product by $MeC(O)Fe(CO)_4^-$ which was formed during the reaction. Both methods give complete reaction within time of mixing. The yellow crystalline product was stable indefinitely under N_2. In solution, however, thermal disruption occurred and the stability was dependent upon cation, as discussed below, and solvent polarity. Solutions of **PPN$^+$1** or **Et$_4$N$^+$1** in acetonitrile, a good donor solvent, decomposed within 1 day while THF solutions were stable approximately 2 days at 22 °C. Synthesis of the chromium heterobimetallic analogue was attempted, but the product was not thermally stable and could not be isolated.

The Structure of $[MeFeW(CO)_9]^-$. The ν(CO) IR band pattern of $MeFeW(CO)_9^-$ (ν(CO) = 2060 (vw), 2004 (mw), 1942 (s), 1909 (m), 1870 (m) cm^{-1}) was identical with that of $HFeW(CO)_9^-$ (ν(CO) = 2063 (vw), 2009 (mw), 1940 (s), 1911 (m), 1870 (m) cm^{-1}), whose structure was described above.[1b] That the spectral similarity signaled a similar structure of the bimetallic was corroborated, albeit incompletely, by X-ray crystallography. A data set was collected for crystals of [PPN][MeFeW(CO)$_9$] and refinement attempted,[11] however severe disorder in the anion prevented a detailed analysis. Although the connectivity of the atoms is not in question, i.e., the two metals are in an octahedral coordination environment, connected via one vertex, a twofold disorder in the metal position and an eightfold disorder in the methyl group's position (among the eight ligand positions cis to the Fe–W bond) rendered the metal ligand bond lengths an uninterpretable average. Thus the only useful metric information in the anion was the M–M distance of 2.880 (1) Å. This distance is consistent with the Fe–W distance in the hydride and triphenylphosphinegold derivatives of $EFeW(CO)_9^-$: 2.997 (2) and 3.012 (3) Å, respectively. The disorder actually prevents the firm conclusion, based on X-ray crystallography, that the Me ligand is on Fe. Nevertheless, the shorter Fe–W distance of the Me derivative is consistent with the idea that the $MeFe(CO)_4^-$ is a better electron-donating metalloligand than is $HFe(CO)_4^-$ or $Ph_3AuFe(CO)_4^-$.

Reactivity of $MeFeW(CO)_9^-$. Stability of the Dimer. In THF solution at 22 °C the Et_4N^+ salt of 1 decomposed over a 24-h period yielding $MeC(O)Fe(CO)_4^-$ and $W(CO)_6$, as shown in eq 4.

$$\underset{\mathbf{1}}{MeFeW(CO)_9^-} \rightarrow \underset{\mathbf{4}}{MeC(O)Fe(CO)_4^-} + W(CO)_6 + [W] \tag{4}$$

A quantitative study of the decomposition by IR spectroscopy showed that 1 equiv of $MeC(O)Fe(CO)_4^-$, and less than 1 equiv of $W(CO)_6$, was produced. The CO required for formation of 4 as well as for the tungsten hexacarbonyl thus results from the decomposition of the $[W(CO)_5]$ fragment.[13]

When the dimer decomposition (eq 4) was carried out in the presence of CO, a more rapid reaction occurred and the yield of $W(CO)_6$ was quantitative. With PPh_3 as the added ligand, the products were $MeC(O)Fe(CO)_3PPh_3^-$ and the mono- and bis-substituted tungsten carbonyls, as indicated in eq 5. The phosphine-substituted iron acyl, i.e., $MeC(O)Fe(CO)_3PPh_3^-$ (**3**), was detected by infrared spectroscopy; however, this decomposed over time to give the tetracarbonyl iron acyl complex **4**. Since **3** decomposed, its stability under the reaction conditions was tested. Infrared monitoring of a CH_3CN solution of **3** showed that after a 70-h period, only 15% decomposition had occurred. In contrast, reaction of **3** with photochemically generated $W(CO)_5{\cdot}THF$ yielded over the course of 3 h **Et$_4$N$^+$ 1**, $W(CO)_6$, $Fe(CO)_3PPh_3W(CO)_5^-$,[14] $W(CO)_5PPh_3$, and $W(CO)_4(PPh_3)_2$ (eq 6). After longer periods the dimeric alkyl decomposed as in eq 4. Thus, the presence of the $W(CO)_5{\cdot}THF$ promoted the decomposition of **3**.

$$\begin{aligned} &MeFeW(CO)_9^- + \text{excess } PPh_3 \rightarrow \\ &\quad \underset{\mathbf{3}}{MeC(O)Fe(CO)_3PPh_3^-} + \underset{30\%}{W(CO)_5PPh_3} + \underset{70\%}{W(CO)_4(PPh_3)_2} \end{aligned} \tag{5}$$

$$\begin{aligned} &MeC(O)Fe(CO)_3PPh_3^- + W(CO)_5{\cdot}THF \rightarrow \\ &\quad MeFeW(CO)_9^- + W(CO)_6 + MeFeW(CO)_8PPh_3^- + \\ &\quad W(CO)_5PPh_3 + W(CO)_4(PPh_3)_2 \end{aligned} \tag{6}$$

It is noteworthy that when photochemically generated $W(CO)_5{\cdot}THF$ was reacted with PPh_3 at room temperature, the product was monosubstituted $(Ph_3P)W(CO)_5$. The fact that large amounts of the disubstituted *cis*- and *trans*-$(Ph_3P)_2W(CO)_4$ are observed in the reactions described by eq 4 and 5 suggests that CO ligands are labilized during the course of the reaction. Since oxygen donor ligands are well-known to "cis-labilize" CO ligands,[16] we suggest that this labilization most likely occurs in an intermediate (vide infra) in which the $W(CO)_5$ Lewis acid is interacting with the anionic metal acylate oxygen. Attempts to mimic this coordination complex have been made by reacting

---

[11] The [PPN][MeFeW(CO)$_9$] salt crystallized as one unique cation–anion pair in the centrosymmetric space group $P2_1/c$. Intensity data were collected on a Nicolet R3m diffractometer employing the θ–2θ scanning technique. A total of 6722 unique reflections were collected. The molecular structure of [PPN][MeFeW(CO)$_9$]: $C_{46}H_{33}O_9P_2NFeW$, M_r 1045.41, monoclinic, a = 16.854 (3) Å, b = 16.357 (3) Å, c = 17.574 (3) Å, β = 114.84 (1)°, V = 4326 (1) Å^3, μ = 32.9 cm^{-1}, T = 20 (1) °C.

[12] Gartzke, W.; Huttner, G. *Chem. Ber.* **1975**, *108*, 1373.

[13] Hyde, C. L.; Darensbourg, D. J. *Inorg. Chem.* **1973**, *12*, 1286.

[14] The phosphine-substituted heterobimetallic alkyls could also be easily synthesized from the addition of 1 equiv of methyl tosylate to [K][PPN][P(OMe)$_3$(CO)$_3$FeW(CO)$_5$] to yield [PPN][P(OMe)$_3$(CO)$_3$Fe(Me)W(CO)$_5$]. IR (ν(CO) in CH_3CN): 2061 (w), 2046 (w), 1955 (sh), 1924 (s), 1896 (w), 1847 (m) cm^{-1}.

[15] Arndt, L. W. Ph.D. Dissertation, Texas A&M University, 1986.

[16] Darensbourg, D. J.; Ovalles, C. *J. Am. Chem. Soc.* **1984**, *106*, 3750 and references therein.

Table I. Kinetic Data for the Reactions of $MeFe(CO)_4^-$ and $MeFeW(CO)_9^-$ with Triphenylphosphine[a]

entry	M	$[PPh_3]$, M	[M], M	temp, °C	k_2,[b] $M^{-1}\ s^{-1}$
1	$[PPN][MeFe(CO)_4]$	0.277	0.0139	25	$(1.4 \pm 0.2) \times 10^{-5}$
2		0.582	0.00970	25	$(1.4 \pm 0.2) \times 10^{-5}$[d]
3		0.971	0.00970	25	$(1.3 \pm 0.6) \times 10^{-5}$[d]
4	$[Na][MeFe(CO)_4]$[c]	0.191	0.00956	25	$(2.6 \pm 0.7) \times 10^{-3}$
5	$[PPN][MeFeW(CO)_9]$	0.198	0.00956	25	$(6.4 \pm 0.5) \times 10^{-4}$[d]
6		0.452	0.00561	25	$(6.4 \pm 0.7) \times 10^{-4}$[d]
7	$[Na][MeFeW(CO)_9]$[c]	0.191	0.00956	25	$(2.2 \pm 0.4) \times 10^{-3}$
8	$[Et_4N][MeFeW(CO)_9]$	0.113	0.00561	10	$(3.8 \pm 0.3) \times 10^{-4}$
9		0.0113	0.0112	25	$(1.4 \pm 0.1) \times 10^{-3}$
10		0.113	0.00561	25	$(1.3 \pm 0.1) \times 10^{-3}$
11		0.118	0.00392	25	$(1.3 \pm 0.1) \times 10^{-3}$[d]
12		0.225	0.00561	25	$(1.3 \pm 0.1) \times 10^{-3}$
13		0.451	0.00561	25	$(1.4 \pm 0.1) \times 10^{-3}$[d]
14		0.938	0.00942	25	$(1.2 \pm 0.2) \times 10^{-3}$[d]
15		0.113	0.00561	30	$(1.8 \pm 0.1) \times 10^{-3}$[d]
16		0.113	0.00561	35	$(2.7 \pm 0.1) \times 10^{-3}$[d]
17		0.113	0.00561	40	$(3.8 \pm 0.3) \times 10^{-3}$[d]

[a] Rate constants are based on an average of two to five kinetic runs, except where noted. All reactions were run in THF. [b] $k_2 = k_{obsd}(av)/[PPh_3]$. The errors for k_2 were determined by a least-squares refinement of the data used for calculating k_{obsd} at the 90% confidence limit. The error in $[PPh_3]$ was calculated by assuming a ±0.001-g error in weight measurements and a ±0.1-mL error in volume. [c] The Na^+ salt was obtained by reacting at least 5 equiv of $NaBPh_4$ with the PPN^+ salt as discussed in the Experimental Section. Two equivalents of $NaBPh_4$ was not enough to effect a complete cation exchange as ascertained by a depression in the rate. [d] The rate constant in this case was based on one kinetic run.

$PPN^+(OC)_5WC(Me)O^-$ with $W(CO)_5{\cdot}THF$. The resulting complex was not isolated, but on the basis of IR spectroscopy and subsequent reaction chemistry, its structure was assumed to be the μ-acyl dimeric anion **6**.

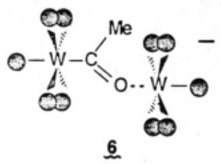

6

The reaction of the assumed dimer **6** with PPh_3 cleanly regenerated (2-h reaction time) the acylate $PPN^+(OC)_5WC(Me)O^-$ along with neutral $Ph_3PW(CO)_5$ and $(Ph_3P)_2W(CO)_4$. The ratio of bis- to mono-substituted neutral complexes was on the order of 1–4. This reaction is similar to that described by eq 6 above; however, with the iron acylate, an intermediate dimeric complex similar to **6** was not observable.

Kinetic Studies of the Reaction of 1 with PPh_3. The reaction described in eq 5 follows a second-order kinetic rate law, i.e., first order in both $MeFeW(CO)_9^-$ and PPh_3 (eq 7). Rate constants for this reaction under varying

$$\text{rate} = k_2[MeFeW(CO)_9^-][PPh_3] \qquad (7)$$

conditions may be found in Table I. The second-order rate constant, k_2, for $\mathbf{Et_4N^+1}$ at 25 °C was $(1.3 \pm 0.1) \times 10^{-3}\ M^{-1}\ s^{-1}$ (entries 9–14). This value is highly dependent on counterion. For example, $\mathbf{PPN^+1}$ exhibited a rate one-half that of $\mathbf{Et_4N^+1}$ (entries 5 and 6), while $\mathbf{Na^+1}$ was about twice as fast as $\mathbf{Et_4N^+1}$ (entry 7). These counterion effects correlate with the order of ion pairing generally found for cations with anionic metal carbonyls: $Na^+ > Et_4N^+ \gg PPN^+$.[17] The rate of reaction for $\mathbf{Et_4N^+1}$ was also found to be dependent on solvent polarity, where rate acceleration was noted in more polar solvents ($CH_3CN > THF$).[18] An Eyring plot of the temperature dependence of k_2 values (Table I, entries 8, 9, 15, 16, 17) is given in Figure 1. The activation parameters thus derived are $\Delta H^\ddagger = 12.9 \pm 0.1$ kcal/mol and $\Delta S^\ddagger = -30 \pm 2$ eu.

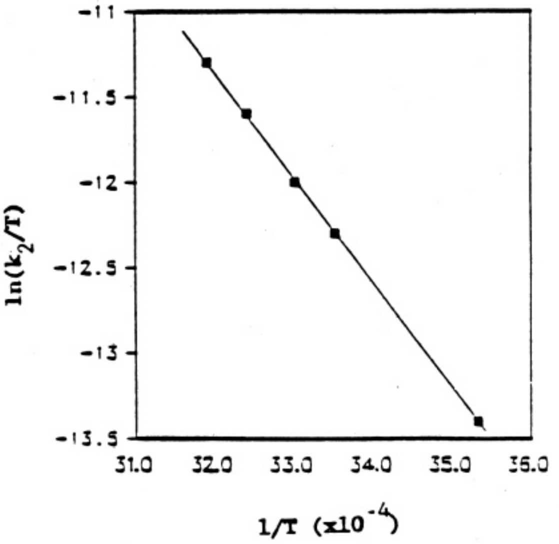

Figure 1. Eyring plot of the kinetic data acquired for the reaction of $[Et_4N][MeFeW(CO)_9]$ with 20 equiv of triphenylphosphine with temperatures ranging from +10 to +50 °C.

Kinetic Studies of the Reaction of 2 with PPh_3. In order to contrast the monomeric and heterobimetallic forms of $MeFe(CO)_4^-$ (**2**), we determined the kinetic parameters of the reaction of PPh_3 with $MeFe(CO)_4^-$. Reaction of **2** with PPh_3 gave $MeC(O)Fe(CO)_3PPh_3^-$, which eventually decomposed to the tetracarbonylacyliron anion and solid iron decomposition products (eq 8). As entries

$$\underset{\mathbf{2}}{MeFe(CO)_4^-} + PPh_3 \xrightarrow{THF} MeC(O)Fe(CO)_3PPh_3^- \rightarrow \underset{\mathbf{4}}{MeC(O)Fe(CO)_4^-} + [Fe] \qquad (8)$$

1–3 in Table I indicate, the reaction obeys a second-order rate expression, first order in each reactant. Entry 4, Table I, indicates a profound counterion effect, with $\mathbf{PPN^+2}$ (entry 1) being 200× slower that $\mathbf{Na^+\ 2}$ (entry 4). These results are consistent with the earlier work of Collman, Brauman, et al. on the reaction of salts of n-$C_{10}H_{21}Fe(CO)_4^-$ and PPh_3 yielding $PPh_3PFe(CO)_3C(O)(n\text{-}C_{10}H_{21})^-$. In that work activation parameters were determined to be $\Delta H^\ddagger = 19.3 \pm 0.6$ kcal/mol and $\Delta S^\ddagger = -19 \pm 2$ eu, and the reaction rate was highly counterion dependent.[7]

The important conclusion regarding comparative studies of $MeFe(CO)_4^-$ and $MeFeW(CO)_9^-$ is that as the PPN^+

---

(17) Darensbourg, M. Y. *Prog. Inorg. Chem.* **1985**, *33*, 221.
(18) Wax, M. J.; Bergman, R. G. *J. Am. Chem. Soc.* **1981**, *103*, 7028.

salts, reaction rates are over an order of magnitude slower for the monomeric than the heterobimetallic complex. Upon exchanging the cation from PPN^+ to Na^+, an enhancement of rate is shown for both reagents; however, the more dramatic effect is on the monomer. In fact, within experimental error, the rates of reaction of $\mathbf{Na^+1}$ or $\mathbf{Na^+2}$ with triphenylphosphine are identical. It is reasonable that the Na^+ ion assists in dimer disruption,[19] forming more stable ion pair interactions with the smaller anion, and allows the reaction with PPh_3 to funnel through the monomer. The promotional effect of alkali cations on migratory insertion is well-known, and the accepted explanation is that an interacting positive charge stabilizes the negative charge accumulating on the acylate oxygen.[20] The promotion of R/CO migratory insertion by main-group Lewis acids has also been firmly established.[21]

Mechanism for Migratory Insertion/Dimer Disruption of $\mathbf{MeFeW(CO)_9^-}$. Members of the family of mixed-metal dimers, $XFeW(CO)_9^-$, have exhibited different rate-determining steps for dimer disruption in the presence of PPh_3.[1b,15] The reaction of $HFeW(CO)_9^-$ with PPh_3 showed a first-order dependence only on the dimer concentration, and $Ph_3PW(CO)_5$ was the major (≥90%) W-containing product. Yet the activation parameters (measured in THF for the Et_4N^+ salts), $\Delta H^\ddagger = 11 \pm 1.2$ kcal/mol and large negative entropy of $\Delta S^\ddagger = -48 \pm 6$ eu, are more indicative of a structural reorganization in the rate-determining step than some bond cleavage step. The $HFe(CO)_3P(OMe)_3Cr(CO)_5^-$ anion, which has a $P(OMe)_3$ ligand substituted for a CO on Fe, trans to the Fe–Cr bond, was found to be much more thermally robust than the nonsubstituted dimers. This was attributed to the additional stability of the Fe→Cr bond brought about by the enhancement of Fe nucleophilicity by the P-donor ligand. Reaction of this anion with PPh_3 also followed a first-order rate expression, rate = $k[HFe(CO)_3P(OMe)_3Cr(CO)_5^-]$, independent of PPh_3 concentration above a fivefold excess of entering ligand. The activation parameters for this reaction were typical for CO dissociation as the rate-determining step: $\Delta H^\ddagger = 27$ kcal/mol and $\Delta S^\ddagger = 3.8 \pm 2$ eu.[15] Consistent with this interpretation were the observed products $HFe(CO)_3P(OMe)_3^-$ and *trans*-$Cr(CO)_4(PPh_3)_2$, which also indicated that triphenylphosphine substituted for CO on the intact dimer, followed by dimer disruption. For all the heterobimetallic, donor–acceptor type complexes that we have investigated, the most likely candidate for simple metal–metal′ bond cleavage in the rate-determining step is the $MnCr(CO)_{10}^-$ anion. Triphenylphosphine reacts with $PPN^+MnCr(CO)_{10}^-$ yielding $Mn(CO)_5^-$ and $Cr(CO)_5PPh_3$, with $\Delta H^\ddagger = 28 \pm 2$ kcal/mol and $\Delta S^\ddagger = 1 \pm 7$ eu.[22]

We have demonstrated that the reaction of $PPN^+MeFeW(CO)_9^-$ with PPh_3 obeys a second-order kinetic expression, first order in each reagent. A comparison of the activation parameters obtained for this reaction, $\Delta H^\ddagger = 12.9 \pm 0.1$ kcal/mol and $\Delta S^\ddagger = -30 \pm 2$ eu, and those above thus are not consistent with either CO dissociation or Fe–W bond cleavage in the rate-determining step. They are in fact closer to the values for the $HFeW(CO)_9^-$ reaction with PPh_3, i.e., the "structural reorganization rate-determining step" reaction. Clearly part of the structural reorganization in the case of **1** is the Me/CO migratory insertion reaction.

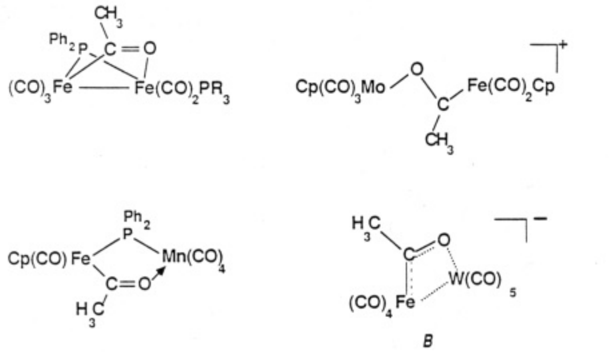

Figure 2. Literature examples of μ_2-acyl complexes (see text for references) as compared to the intermediate proposed for the reaction of $MeFeW(CO)_9^-$ with triphenylphosphine (B).

Scheme I

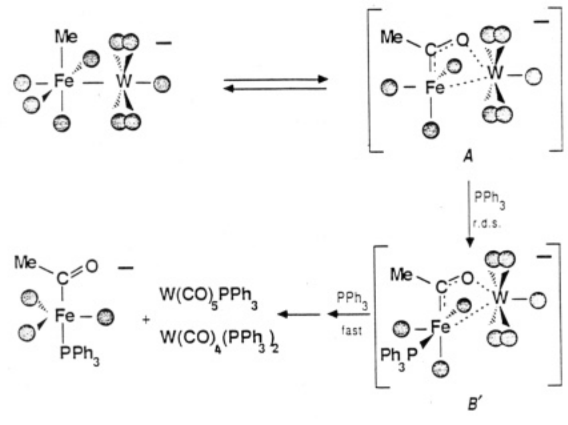

The mechanism for reaction of **1** with PPh_3 depicted in Scheme I is consistent with the above observations. An equilibrium migratory insertion process followed by a rate-determining addition of the PPh_3 to the open site resulting from the CO insertion is proposed. The proposed intermediate species includes the reasonable assumption that the $W(CO)_5$ fragment may act as a Lewis acid to the acyl oxygen atom (vide supra), a factor which enhances the migratory insertion rate. The exact position of PPh_3 addition is not obvious. As was shown by ^{13}C CO-labeling experiments, the carbonyl groups on the heterobimetallic methyl compound are extremely labile. Attempts to label the carbonyl groups of $\mathbf{PPN^+1}$ on one metal center ($W(^{13}CO)_5$) resulted in scrambling throughout **1** (i.e., $MeFeW(^*CO)_9^-$). Similar ligand scrambling may occur during the migratory insertion process. Dimer disruption then occurs, and the monometallic fragments rapidly scavenge ligands (such as CO or PPh_3) to fill their open coordination sites. This results in the product distribution shown in eq 5. The carbonyl ligand in the resulting iron acyl complex **4** most likely is derived from decomposition of the $W(CO)_5$ fragment.

The proposed intermediate species, labeled A and B in Scheme I, were modeled making use of the *Molecular Editor Program*.[23] The molecular structure of $HFeW(CO)_9^-$ was modified such that an acyl group was created by using values for bond lengths and bond angles based on average values derived from the literature as follows: Fe–C(acyl) = 2.006 Å; C(acyl)–O = 1.17 Å; C(acyl)–CH_3 = 1.46 Å; W–O = 1.83 Å; ∠Fe–C–O = 125.7°; ∠Fe–C–CH_3 = 115.8°; and ∠CH_3–C–O = 118.5°. The $W(CO)_5$ unit was then slipped from strictly Fe–W interaction to the si-

---

[19] Fachinetti, G. *J. Chem. Soc., Chem. Commun.* **1979**, 396.

[20] (a) Berke, H.; Hoffmann, R. *J. Am. Chem. Soc.* **1978**, *100*, 7224. (b) Collman, J. P.; Winter, S. R. *J. Am. Chem. Soc.* **1973**, *95*, 4089.

[21] Butts, S. B.; Holt, E. M.; Strauss, S. H.; Alcock, N. W.; Stimson, R. E.; Shriver, D. F. *J. Am. Chem. Soc.* **1979**, *101*, 5864.

[22] Park, Y. K. Ph. D. Dissertation, Texas A&M University, 1986.

[23] The *Molecular Editor Program* software-based modeling program developed by A. Smith, Drexel University, Philadelphia, PA, 1986.

multaneous interaction of Fe and acyl oxygen as shown in Figure 2. The choice of a W–O distance of 1.83 Å resulted in a W–Fe distance of 3.76 Å, i.e., beyond the possibility of a bonding interaction. The point of these modeling studies was that there are no prohibitive steric repulsions due to ancillary CO ligands in such proposed intermediates.

The likelihood of such an intermediate is further supported by isolated species documented by structural analyses in the literature (Figure 2). Especially pertinent is the dinuclear species $(CO)_3Fe(\mu\text{-}PPh_2)(\mu\text{-}C(O)Me)Fe(CO)_2PR_3$, with an Fe–Fe distance of 2.654 (1) Å, which forms an Fe(1)–C acyl bond (1.962 (7) Å) and an Fe(2)–O bond (2.013 (4) Å).[24] Heterobimetallic species with bridging acylates have also been isolated. A crystal structure of $CpFe(CO)_2(\mu\text{-}C(O)Me)Mo(CO)_3Cp^+SbF_6^-$ reveals a Mo–O bond length of 2.158 (8) Å and an Fe–C bond length of 1.96 (1) Å for the bridging ligand, as shown below.[25] There was no metal–metal′ contact distance in this complex. The heterobimetallic species $Cp(CO)Fe(C(O)Me)(\mu\text{-}PPh_2)Mn(CO)_4$ looks very much like the proposed intermediate A with the acylate bridging the two metal centers with a partial interaction with the manganese center.[26] The Fe–C bond length was 1.919 (8) Å and the Mn···O distance was 2.024 (5) Å indicative of a bonding interaction. There was no metal–metal′ bond present as the distance between the two metals was 3.718 (1) Å.

Comparison of Small Molecule Reactions with the Heterobimetallic and Monomeric Alkyl. The methyl migratory insertion reaction may also be enhanced by the addition of CO. For $\mathbf{Et_4N^+1}$ + CO, the dimer disruption was faster than in the presence of added PPh_3. The products observed were the tetracarbonyliron acyl and tungsten hexacarbonyl. A similar situation exists for the monomer; reaction of $\mathbf{PPN^+2}$ with CO results in the formation of $\mathbf{PPN^+4}$.

Although a sample of $\mathbf{PPN^+2}$ dissolved in THF showed no reaction under 600 psi of CO_2, reaction of 1 with 1 atm of CO_2 (eq 9) gave good yields of acetatopentacarbonyltungsten (0).[10] Since the monomer $MeFe(CO)_4^-$ was unreactive with CO_2, a role for reactivity of the intact heterobimetallic followed by acetate transfer to the $W(CO)_5$ moiety is indicated.

$$MeFeW(CO)_9^- + CO_2 \rightarrow MeOC(O)W(CO)_5^- + [Fe] \quad (9)$$

In fact a model for the reasonable mixed metal intermediate for CO_2 reaction with 1 was obtained from studies with CS_2. Reaction of $MeFeW(CO)_9^-$ with CS_2 (eq 10) occurred within 20 min to quantitatively yield a product whose elemental analysis, mass spectrum, and IR and NMR spectral data are consistent with those of the formulation $(\mu\text{-}MeCS_2)FeW(CO)_8^-$ (**5**).[27]

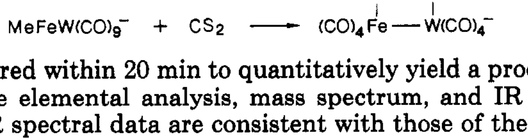

$$MeFeW(CO)_9^- + CS_2 \longrightarrow (CO)_4Fe(\mu\text{-}S_2CMe)W(CO)_4^- \quad (10)$$

The reaction of acids with the alkyl species provided similar results for both the monomer and dimer. Addition of acids, such as CH_3COOH or HCl, to 1 or 2 readily cleaved the Fe–Me bond within time of mixing to generate methane with no acetaldehyde or other side products detected in the GC. Addition of methylating agents such as MeI or MeOTs yielded products of migratory insertion for both 1 and 2, producing acetone instead of ethane. Some methane was also produced in both cases. Both reactions occurred within time of mixing.

Summary and Comments

The above represents the second reactivity study of $XFeM(CO)_9^-$ anions which contrasted the reactive Fe–X functionality in a heterobimetallic with its monomeric $XFe(CO)_4^-$ analogue. In the first such study of X = H,[1] the diagnostic catalytic olefin isomerization reaction demonstrated that the enhanced CO lability of the bimetallic $HFeM(CO)_9^-$ as contrasted to $HFe(CO)_4^-$ could account for greater rates of catalysis by the former.[6] The typical reversible M–H/olefin insertion mechanism was found to be operative for both.

The current reactivity study examined reactions of the $MeFeW(CO)_9^-$ anion. Iron-based Me/CO migratory insertion in the intact dimer was concluded to be the rate-determining step in reactions with nucleophiles such as PR_3 which ultimately led to dimer disruption. It was found that the Me/CO migratory insertion reaction in both $MeFeM(CO)_9^-$ and $MeFe(CO)_4^-$ is promoted by the presence of nucleophiles (PR_3 and polar solvents),[28] and electrophiles (Na^+ or, in the case of the heterobimetallic, $W(CO)_5$) also promoted the reaction. The role of the heterobimetallic is to furnish an internal, readily available transition-metal Lewis acid, $W(CO)_5$, which assists in the migratory insertion process by interacting at the acyl oxygen site. That the 16-electron $W(CO)_5$ Lewis acid is indeed involved in such a process was ascertained by the effect on CO lability that the interacting acyl oxygen ligand has on $W(CO)_5$.

It is noteworthy that earlier, analogous dimer disruption studies on reactions of $HFeW(CO)_9^-$ with PPh_3 did not produce evidence for the $Ph_3PFe(CO)_3CHO^-$ or a heterobimetallic formyl as intermediate. The rate of reaction followed a simple first-order dependence on $[HFeW(CO)_9^-]$, independent of PPh_3 concentration at $[PPh_3]/[HFeM(CO)_9^-]$ ratios > 5, and the monosubstituted $Ph_3PW(CO)_5$ and $HFe(CO)_4^-$ were the sole organometallic products.[1] Nevertheless the activation parameters for the heterobimetallic hydride of $\Delta H^{\ddagger} = 11 \pm 1.2$ kcal/mol and $\Delta S^{\ddagger} = -48 \pm 6$ eu are similar to those for the $MeFeW(CO)_9^-$ anion ($\Delta H^{\ddagger} = 12.9 \pm 0.1$ kcal/mol and $\Delta S^{\ddagger} = -30 \pm 2$ eu) reported here. We suggest that a structural reorganization of both intact dimers is involved in the rate-determining step. In the case of $MeFeW(CO)_9^-$, that structural reorganization was reasonably established to be $W(CO)_5$ migration to the acyl oxygen.

Although a similar heterobimetallic formyl intermediate has not been completely ruled out in the analogous hydride, the more likely precursor to dimer disruption involves migration of the $W(CO)_5$ unit to the hydride site, generating a transient $Fe\text{–}H{:}\rightarrow W(CO)_5$ moiety. Clearly subtle differences in electron distributions and accessible sites for electrophile interaction lead to discernible dif-

---

[24] Yu, Y.-F.; Gallucci, J.; Wojcicki, A. *J. Organomet. Chem.* **1983**, *251*, 227.

[25] Sunkel, K.; Nagel, U.; Beck, W. *J. Organomet. Chem.* **1980**, *187*, 9.

[26] Rosen, R. P.; Hoke, J. B.; Whittle, R. R.; Geoffroy, G. L.; Hutchinson, J. P.; Zubieta, J. A. *Organometallics* **1984**, *3*, 846.

[27] Mass spectrum (FAB on a Kratos MS-50TA from a nitrophenyl octyl ether matrix) of anion showed base peak at *m/e* 554 (expected *m/e* 555.2 for $MeCS_2FeW(CO)_8^-$) as well as successive loss of eight CO's. Although the possibility that the $MeCS_2$ ligand resides in only one metal center cannot be ruled out, the robust nature of this heterobimetallic, compared to other substituted heterobimetallics, suggests a ligand-bridge supported metal–metal bond.

[28] In contrast, $Ph_3P{=}O$ did not act as a promoter to increase the rate of migratory insertion as has been seen observed for neutral metal alkyl systems.[29]

[29] Webb, S. L.; Giandomenico, C. M.; Halpern, J. *J. Am. Chem. Soc.* **1986**, *108*, 345.

ferences in reaction pathways.

Acknowledgment. This work was supported with funds from the National Science Foundation (CHE-8603664). C.M.K. and K.E.V. were undergraduate fellows of the Robert A. Welch Foundation whose support is gratefully acknowledged.

Registry No. **Et_4N^+1**, 113724-94-0; **Na^+1**, 113724-95-1; **PPn^+1**, 113669-28-6; **Et_4N^+2**, 113669-30-0; **Na^+2**, 64883-59-6; **PPN^+2**, 113669-31-1; **Et_4N^+3**, 113669-33-3; **Na^+3**, 113669-41-3; **PPN^+3**, 113669-40-2; **PPN^+4**, 36464-58-1; **Et_4N^+5**, 113669-39-9; $[PPN]_2[FeW(CO)_9]$, 99604-07-6; $[Et_4N]_2[FeW(CO)_9]$, 99559-70-3; $W(CO)_5{\cdot}THF$, 36477-75-5; $[PPN][HFe(CO)_4]$, 56791-54-9; $Fe(CO)_4^{2-}$, 22321-35-3; $[Et_4N][HFe(CO)_4]$, 25879-01-0; $[K][PPN][P(OMe)_3(CO)_3FeW(CO)_5]$, 113669-35-5; $[PPN][P(OMe)_3(CO)_3Fe(Me)W(CO)_5]$, 113669-37-7; $W(CO)_6$, 14040-11-0; $W(CO)_5OC(O)CH_3^-$, 45146-15-4; $[PPN][W(CO)_5I]$, 81315-55-1; $MeFe({*}CO)_4W({*}CO)_5^-$, 113669-27-5; $Na[MeC(O)Fe(CO)_4]$, 64867-63-6.

Synthesis and Molecular Structure of $(\eta^5\text{-}C_5Me_5)_2Hf(H)(NHMe)$. Structural Evidence for Nitrogen-to-Hafnium π-Donation

Gregory L. Hillhouse,[1] A. Ray Bulls, Bernard D. Santarsiero, and John E. Bercaw*

Division of Chemistry and Chemical Engineering, California Institute of Technology,[†]
Pasadena, California 91125

Received August 31, 1987

$Cp^*_2HfH_2$ ($Cp^* = \eta^5\text{-}C_5Me_5$) reacts with excess methylamine to afford the formally 16-electron complex $Cp^*_2Hf(H)(NHMe)$ (**2**), which has been crystallographically characterized. Crystals of **2** were grown from a cold petroleum ether solution and crystallized in space group $P2_12_12_1$ with $Z = 4$, $a = 8.601$ (4) Å, $b = 14.030$ (6) Å, and $c = 17.145$ (4) Å. The least-squares refinement converged to $R(F) = 0.034$ for 3610 unique data with $I > 0$. Complex **2** adopts an orientation about the amido nitrogen which is consistent with π-donation of the nitrogen's lone pair of electrons to the hafnium center: the methylamido moiety is essentially planar about nitrogen with the amido methyl group directed toward one Cp* ring and the amido hydrogen directed toward the other ring. Variable-temperature NMR studies place an upper limit of about 10 $kcal{\cdot}mol^{-1}$ on the strength of this Hf–N π-interaction. These results support the correlation between the hydride chemical shift (^1H NMR) in complexes of the formula $Cp^*_2Hf(H)(X)$ and the degree of X-to-hafnium π-donation: increasing π-donation leads to higher field chemical shifts. Thus, the observation that the hydride ligand in $Cp^*_2Hf(H)(NMe_2)$ (**3**) resonates at δ 11.2 (compared to δ 9.2 for $Cp^*_2Hf(H)(NH_2)$ (**1**) and δ 9.1 for **2**) suggests that steric congestion between the amido methyl groups and the Cp* rings prevents the dimethylamido moiety of **3** from adopting the orientation necessary for effective N-to-Hf π-donation.

Introduction

In the course of our studies of the chemistry of permethylhafnocene derivatives we have encountered and commented on unusual spectral characteristics of amido complexes of the type $Cp^*_2Hf(H)(NR'R'')$ ($Cp^* = \eta^5\text{-}C_5Me_5$; R′, R″ = H, alkyl, aryl, diazo).[2] Specifically, we were intrigued by the observations that most compounds of this class exhibit ^1H NMR spectra inconsistent with the molecular geometry required for effective π-overlap between the nitrogen lone pair and an appropriate empty, low-lying orbital of the $[Cp^*_2Hf(H)]$ fragment, even though it is generally assumed that hard π-donor ligands like OR^-, NR_2^-, and F^- form strong π-bonds with early transition metals when orbital interactions allow.[3,4] Moreover, in the absence of such a Hf–N π-interaction these complexes are electronically unsaturated, 16e species. It seemed clear that elucidation of the nature and extent of π-bonding in these and related systems was essential to understanding (and predicting) the structures and reactivities of such species. The two limiting geometries for a $Cp^*_2Hf(H)(NR'R'')$ molecule containing a planar amido moiety are illustrated in Figure 1. Structure A (where Hf–N π-bonding is maximized) is electronically preferred over structure B (where the N lone pair is orthogonal to the metal fragment's LUMO or proper π-symmetry),[5] but B is clearly a sterically more favorable geometry than is A (in A, R′ and R″ are oriented toward the bulky Cp* rings; in B this steric congestion is minimized).[6,7] Herein we present the results of an X-ray structural study of one

---

[†] Contribution no. 7657.

[1] Present address: Department of Chemistry, The University of Chicago, Chicago, IL 60637.

[2] (a) Hillhouse, G. L.; Bercaw, J. E. *Organometallics* **1982**, *1*, 1025. (b) Hillhouse, G. L.; Bercaw, J. E. *J. Am. Chem. Soc.* **1984**, *106*, 5472. (c) Roddick, D. M.; Fryzuk, M. D.; Seidler, P. F.; Hillhouse, G. L.; Bercaw, J. E. *Organometallics* **1985**, *4*, 97.

[3] For a good discussion of orbital constraints and symmetry requirements of the bent metallocene derivatives, see: Lauher, J. W.; Hoffmann, R. *J. Am. Chem. Soc.* **1976**, *98*, 1729.

[4] (a) Cardin, D. J.; Lappert, M. F.; Raston, C. L. *Chemistry of Organo-Zirconium and -Hafnium Compounds*; Ellis Horwood Ltd.: West Sussex, 1986. (b) Wailes, P. C.; Coutts, R. S. P.; Weigold, H. *Organometallic Chemistry of Titanium, Zirconium, and Hafnium*; Academic: New York, 1974. (c) Marsella, J. A.; Moloy, K. G.; Caulton, K. G. *J. Organomet. Chem.* **1980**, *201*, 389.

[5] Extended Hückel calculations on the parent $(\eta^5\text{-}C_5H_5)_2Hf(H)(NH_2)$ system show structure A to be 0.51 eV more stable than B. A is 0.87 eV more stable than a third hypothetical structure having a pyramidal amido group. Hoffman, D.; Hoffmann, R., private communication.

[6] Simple close-contact calculations were carried out[6a] for idealized structures A and B on a $Cp^*_2Hf(H)(NHMe)$ model by using standard $[Cp^*_2M(H)X]$ fragment parameters (from the structure of $Cp^*_2Zr(H){\cdot}(OCH{=}WCp_2))$[6b] and the following approximated intramolecular distances: Hf–N = 2.04 Å; Hf–H = 1.90 Å; N–C = 1.47 Å; C–H = 1.09 Å; N–H = 1.02 Å. Angles were 120° about N and tetrahedral about the amido methyl. These calculations showed severe intramolecular nonbonded contacts (<0.6 Å) between the amido Me hydrogens and ring Me hydrogens for A; these close contacts were considerably relieved by rotation about the Hf–N bond and were minimized in the B conformation having the amido Me directed toward the hydride ligand (i.e., R′ = Me and R″ = H), the closest Me–Me contact being 2.1 Å; this was better than the B conformation that has R′ = H and R″ = Me (here the closest Me–Me contact was 1.2 Å). (a) Miller, G. J., private communication. (b) Wolczanski, P. T.; Threlkel, R. S.; Santarsiero, B. D. *Acta Crystallogr. Sect. C: Cryst. Struct. Commun.* **1983**, *C39*, 1330.

0276-7333/88/2307-1309$01.50/0